IEEE Access
Multidisciplinary | Rapid Review | Open Access Journal

Received January 18, 2021, accepted February 9, 2021, date of publication February 15, 2021, date of current version February 24, 2021.

Digital Object Identifier 10.1109/ACCESS.2021.3059443

Intelligent Traction Control Method Based on Model Predictive Fuzzy PID Control and Online Optimization for Permanent Magnetic Maglev Trains

YAHUI LIU, (Student Member, IEEE), KUANGANG FAN, (Member, IEEE), AND QINGHUA OUYANG, (Graduate Student Member, IEEE)

School of Electrical Engineering and Automation, Jiangxi University of Science and Technology, Ganzhou 341000, China
Magnetic Suspension Technology Key Laboratory of Jiangxi Province, Jiangxi University of Science and Technology, Ganzhou 341000, China

Corresponding author: Kuangang Fan (kuangangfriend@163.com)

This work was supported in part by the National Natural Science Foundation of China under Grant 61763018, in part by the 03 Special Project and 5G Program of Science and Technology Department of Jiangxi Province under Grant 20193ABC03A058, in part by the Key Foundation of Education Committee of Jiangxi Province under Grant GJJ170493 and Grant GJJ190451, and in part by the Program of Qingjiang Excellent Young Talents of the Jiangxi University of Science and Technology.

ABSTRACT Considering that the speed control system of the suspended permanent magnetic maglev train is more complicated and the parameters are more unstable than those of other trains, the traditional speed-tracking algorithm has large tracking errors, frequent controller output changes, high energy consumption, and decreasing the passengers' riding comfort. To improve the shortcomings of the traditional automatic train operation (ATO) control algorithm, this paper proposes a predictive fuzzy proportional-integral-derivative control algorithm with weights (WM-F-PID). The main contribution of this work is to propose a cascaded predictive fuzzy PID (F-PID) control algorithm architecture with weights and use an improved steepest descent method to calculate online the weight of the F-PID controller input occupied by the predictive controller output. Compared with the proportional-integral-derivative (PID), F-PID, model predictive control (MPC), and simple cascade predictive fuzzy PID (M-F-PID) control algorithms, this control algorithm effectively improves train tracking accuracy and comfort and reduces train energy consumption and stopping errors.

INDEX TERMS Suspended permanent magnetic maglev train, WM-F-PID control algorithm, online optimization algorithm, speed-tracking.

I. INTRODUCTION

In recent years, the research on the automatic train operation (ATO) technology has also yielded outstanding achievement together with the advances in computer and sensor technologies. ATO for suspended permanent magnetic maglev trains involves a series of technologies such as train speed curve optimization and speed curve tracking, among which speed curve tracking is a key step of ATO technology [1]–[4]. Speed-tracking tracks the expected speed of the train by controlling the traction or braking force of the train. Accurately tracking the ideal speed curve is beneficial to not only improving the parking accuracy of the train but also helps to improve the passengers' riding comfort and reduce the energy consumption of the train. [5]–[7].

To date, extensive research has been conducted on ATO speed-tracking control [8]–[10]. Most of the early speed-tracking controllers were developed based on classical control theory. For example, the PID control algorithm has been widely used due to its simple structure and easy implementation [11]. However, once the PID controller parameters are determined, they cannot be changed in real-time. When the train operation is severely disturbed, the deviation of the system will increase, which is not conducive to saving energy in the train control system, improving passengers' riding comfort, or extending service life. To overcome the disadvantage of not being able to adjust the parameters of the PID control algorithm in real-time, [12] and [13] proposed a

The associate editor coordinating the review of this manuscript and approving it for publication was Huaqing Li.

train speed-tracking control algorithm that combines PID and a fuzzy control algorithm, which can adjust the parameters of PID controller in real-time according to external disturbances. To improve the robustness of the fuzzy PID control algorithm, Yang *et al.* [14] proposed a multimodal fuzzy PID control algorithm. With the development of intelligent control algorithms, a series of intelligent control algorithms has been proposed [15]–[23]. However, these methods rely on the instantaneous state response of the system and cannot predict the future behavior of the system, and perform poorly on systems with large time delays. For this reason, predictive control has become an attractive control algorithm. For instance, [24]–[26] proposed a fuzzy predictive control algorithm, which can effectively improve the passengers' riding comfort. To reduce large tracking error shortcomings, Liu, Wang, and others used the method of online adjustment of the predictive control softness factor to effectively improve the accuracy of train speed-tracking [27], [28]. Chu, Yu *et al.* used the gray prediction GM (1, 1) model to design a train speed-tracking controller, which also effectively improved the speed-tracking accuracy [29]. In recent years, with improvements in computer performance, people have conducted extensive research on the application of Model Predictive Control (MPC) in auto-driving path tracking and train operation optimization and have achieved good results [30]–[32]. However, the calculation efficiency, system response speed, and anti-interference ability of pure predictive control algorithms in practical applications may not be satisfactory.

In summary, when the speed control system input for a suspended permanent magnet maglev train is only the ideal speed, the output error of the speed controller is relatively large due to the system time lag. When the speed control system input for a suspended permanent magnet maglev train is only the predicted speed, the slow response speed of the system and the uncertainty of interference during operation will also cause larger errors. Therefore, the train speed-tracking controller input should not only include ideal speed information but also consider future speed information from the train. Compared with existing work, this paper proposes a new train speed-tracking control architecture that contains two layers of control algorithms: the first layer is a predictive control algorithm, and the second layer is a fuzzy PID control algorithm. The input for the fuzzy PID control algorithm is a combination of predictive control algorithm output and ideal input according to a specific weight. According to the above analysis, the main work of this article is summarized as follows:

1) To solve the problems of the inability of the current train speed control algorithm to predict future behavior and of the poor performance of the system time delay, a WM-F-PID control algorithm is proposed. The control algorithm is composed of three main parts: a predictive control algorithm for the outer layer to make the system include future speed information, and the fuzzy PID feedback control of the inner layer to suppress the uncertain interference and the online weight solution.
2) To solve the problem of the weight of the predictive controller output to the F-PID controller, a novel on-line optimization algorithm of the steepest descent method is proposed to improve the adaptability and real-time performance of the controller on different trains.

The rest of this paper is organized as follows. In Section II, we establish a dynamic model for the train and four indexes for performance evaluation. Section III presents a WM-F-PID speed controller design for suspended permanent magnetic maglev trains and an online optimization algorithm for weight value. In Section IV, the WM-F-PID performance is analyzed in detail by using field data collected in an actual speed-limit section and compared with the function of PID, F-PID, MPC, and simple cascade M-F-PID. Last, conclusions are provided in Section V.

II. TRAIN CONTROL MODEL AND PROBLEM STATEMENT

In Subsection A, we briefly introduce the dynamic train model, which can be roughly divided into traction, inertia, and braking states in accordance with the different running states of the train. Then, four model evaluation and robustness indexes of the control system are considered and proposed in Subsection B, given many uncertain factors in the train control process.

A. TRAIN CONTROL MODEL

Although the train operating conditions are complex, the focus of this article is on the control of the speed-tracking of the train. Therefore, this article adopts the single-mass train model [33]–[35]. Its force is shown in Figure 1. M is the total weight of the train and passengers, g is the acceleration due to gravity, F is the traction force of the train, F_w is the sum of running resistance, N is the levitation force given to the train by the permanent magnet rail, and θ is the gradient of the train track. The model expression is as follows:

$$\begin{cases} \dot{d} = v = \dfrac{\partial d}{\partial t} \\ \ddot{d} = a = \dfrac{\partial v}{\partial t} \\ a = \dfrac{F_r}{M} \end{cases} \tag{1}$$

where d is the train displacement, v is the current speed of the train, t is the running time, a is the acceleration of the train, and F_r is the resultant force of the train. Owing to the different motion states of the train, F_r can be expressed as follows:

$$\begin{cases} F_r = F - F_w - F_b \\ F_r = -F_w \\ F_r = -F_w - F_b \end{cases} \tag{2}$$

where F_b is the braking force of the train, and F_w is the resistance of the train. F_w includes the following parts:

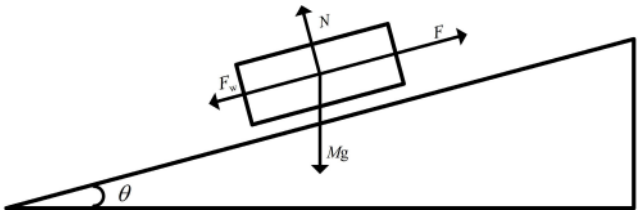

FIGURE 1. Force condition of an urban rail train.

- *Air resistance* F_a

$$F_a = \frac{1}{2} C_d \rho V^2 S_c \tag{3}$$

where C_d is the air-assist coefficient, ρ is the air density, V is the air velocity relative to the train direction, and S_c is the windward area of the train head.

- *Slope resistance* F_s

According to Figure 1, the slope resistance can be expressed as:

$$F_s = Mg \sin\theta \tag{4}$$

where M is the total weight of the train and passengers, g is the acceleration due to gravity, and θ is the gradient of the train track. Given that θ is considerably small, $\sin\theta$ can be approximately equal to θ, then:

$$F_s = Mg \sin\theta \approx Mg\theta \tag{5}$$

F_s can be positive (uphill), negative (downhill),and Zero(no ramp).

- *Curve resistance* F_c

$$F_c = \frac{600g}{r} \tag{6}$$

where r is the turning radius.

Based on the system identification theory of the least square method [36], the equivalent transfer function of the suspended permanent magnetic maglev train is as follows:

$$G(s) = \frac{0.07128}{(s + 0.0954)(s + 0.34)} \tag{7}$$

B. PERFORMANCE EVALUATION INDEX OF CONTROLLER

Several quantitative performance indicators are set here to evaluate the advantages and disadvantages of the method in this paper intuitively and accurately. These indicators include train energy consumption W, energy consumption per unit of quality E_p [16], passenger comfort C_r [37], parking error E_u, and a number of train state changes N_c.

- *Train energy consumption(W)*

$$W = \int_0^{t_r} Fv(t)\, dt = \int_0^{t_r} M\, |a|\, v(t)\, dt \tag{8}$$

where F is the traction force of the train, $v(t)$ is the train speed, and t_r is the total running time, M is the total weight of the train and passengers, a is the acceleration of the train.

The train energy consumption can be approximately discretized as follows:

$$W = \sum_{i=1}^{N} M\, |a_i|\, v_i \Delta t \tag{9}$$

where i is the sampling time, a_i is the acceleration of i^{th} sampling time, v_i is the train speed, and Δt is the sampling interval.

The quality of the same train also changes with passengers getting on and off the train due to the different quality of different types of trains. To compare the energy consumption of different types of trains, the energy consumption per unit mass is defined as follows:

$$E_p = \frac{W}{M} = \int_0^{t_r} |a|\, v(t)\, dt \approx \sum_{i=1}^{N} |a_i|\, v_i \Delta t \tag{10}$$

- *Passenger comfort*(C_r)

$$C_r = \frac{1}{t_r - 1} \sum_{i=1}^{t_r - 1} \left| \frac{a_{i+1} - a_i}{\Delta t} \right| \tag{11}$$

where t_r is the total sampling time, a_i is the acceleration of i^{th} sampling time, a_{i+1} is the acceleration of $(i+1)^{th}$ sampling time,and Δt is the sampling interval.

- *Parking error*(E_u)

$$E_u = |S_i - S_r| \tag{12}$$

in the expression, S_i is the distance between the train stop lines specified between two stations, and S_r is the distance between the actual train stop lines between two stations.

- *Number of train state changes*(N_c)

The running process of the train mainly includes an accelerated traction state, nonoperating inert state, constant speed state, and braking state. The train control system implements safe and efficient train operation by switching back and forth among these operating states. However, the frequent changes in the train running state reduce the train control system service life, increase the energy consumption of the train, and are not conducive to the passengers' riding comfort. Therefore, in this paper, the number of changes in the train running state is taken as a performance index to evaluate the quality of the train control system, which is expressed by N_c here.

III. DESIGN OF SPEED CONTROLLER

In this section, we design a hybrid WM-F-PID cascade controller, considering many uncertain factors in train operation, and the schematic is shown in Figure 2. The inner layer of the controller adopts the most widely used PID controller. However, once the parameters of the PID controller

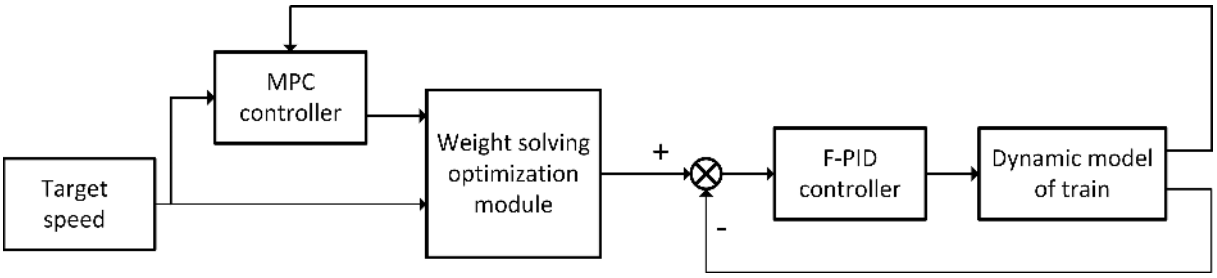

FIGURE 2. The structure of WM-F-PID controller system.

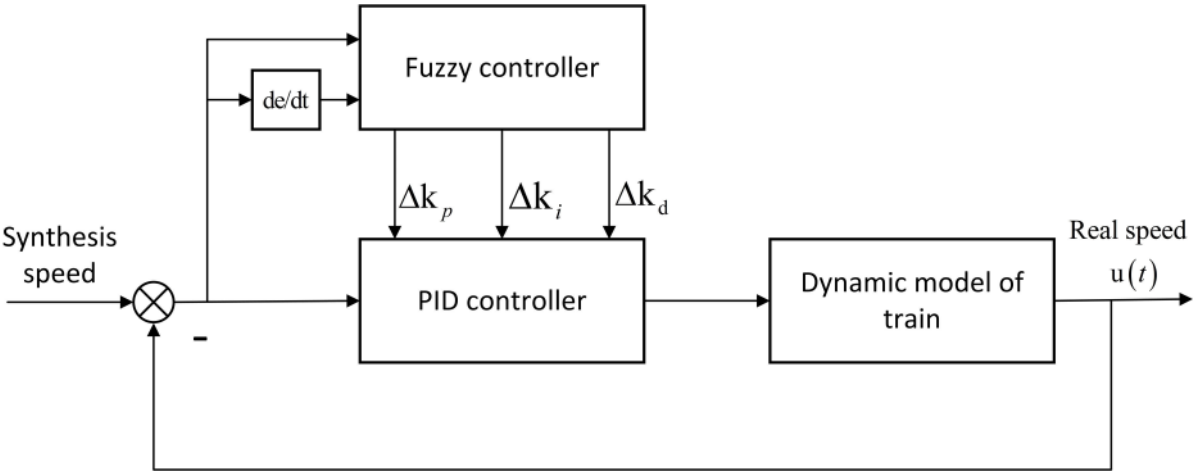

FIGURE 3. Principle diagram of the F-PID controller.

are determined, they cannot be changed during operation. When the system is subjected to various disturbances, its stability decreases. To solve this problem, this paper introduces fuzzy control and uses the driving experience to write fuzzy control rules. Hence, when the train is subjected to various disturbances in the running process, the parameters of the PID controller are adjusted in real-time to improve the robustness of the system. Given that the system has a certain time lag, the input of the F-PID controller is the lag state of the system, leading to deviations in the control system. This paper introduces a predictive controller and uses the predictive controller to predict the system state in the next few sampling times, a certain weight combination of the current and predicted states as the input of the control system, and an online optimization algorithm to solve the optimal weight value. As a result, the system has certain predictive information, and the effect of system lag is reduced. The ideal speed curve of the train can be tracked accurately during operation, and the robustness of the system is improved.

A. DESIGN OF F-PID CONTROLLER

The structure of the F-PID controller of the train speed control system is shown in Figure 3. The system input is the mixed speed obtained by the combination of the predictive controller and the ideal speed according to a certain weight. The feedback into the system is the real-time speed of the train. The two-dimensional fuzzy controller adopts the form of two inputs and three outputs, in which the inputs are the system error e and the system error rate of change ec, and the outputs are ΔK_p, ΔK_i, and ΔK_d, which are used to adjust the parameters of the PID controller in real-time. The real-time parameters of the controller can be expressed as $K_p{}' = K_p + \Delta K_p$, $K_i{}' = K_i + \Delta K_i$, and $K_d{}' = K_d + \Delta K_d$. e and ec are defined as $[-13, 13]$ in the fuzzy domain. In accordance with the accuracy requirements, the fuzzy subset is divided into seven grades $[NB, NM, NS, ZO, PS, PM, PB]$, which refer to negative big, negative medium, negative small, zero, positive small, positive medium, and positive big, respectively. The domains of ΔK_p, ΔK_i, and ΔK_d are $[-13, 13]$, $[-5, 5]$, and $[-1, 1]$, respectively. The fuzzy subset is also graded $[NB, NM, NS, ZO, PS, PM, PB]$. The membership function is a triangular membership function with high sensitivity, the fuzzy reasoning is Mamdani reasoning, and the center of gravity method is adopted in defuzzification. The fuzzy control rules are composed of the knowledge base summarized by excellent drivers' driving experience. The control rules of the fuzzy controller output ΔK_p, ΔK_i, and ΔK_d based on the adjustment rules of the parameters of the PID controller are shown in Tables 1-3.

TABLE 1. Fuzzy rules of ΔK_p.

e \ ec	NB	NM	NS	ZO	PS	PM	PB
NB	PB	PB	PM	PM	PS	ZO	ZO
NM	PB	PB	PM	PS	PS	ZO	NS
NS	NS	PM	PM	PS	ZO	NS	NS
ZO	ZO	PM	PM	PS	ZO	NS	NM
PS	PS	PS	PS	ZO	NS	NS	NM
PM	PS	ZO	NS	NM	NM	NM	NM
PB	ZO	ZO	NM	NM	NM	NB	NB

TABLE 2. Fuzzy rules of ΔK_i.

e \ ec	NB	NM	NS	ZO	PS	PM	PB
NB	ZO	ZO	ZO	ZO	ZO	ZO	ZO
NM	NM	NM	NS	NS	NS	ZO	ZO
NS	NB	NM	NS	NS	ZO	PS	PS
ZO	NB	NM	NS	ZO	PS	PM	PB
PS	NS	NS	ZO	PS	PS	PM	PB
PM	ZO	ZO	PS	PS	PS	PM	PM
PB	ZO	ZO	ZO	ZO	ZO	ZO	ZO

TABLE 3. Fuzzy rules of ΔK_d.

e \ ec	NB	NM	NS	ZO	PS	PM	PB
NB	PS	NS	NB	NB	NB	NM	PS
NM	PS	NS	NB	NM	NM	NS	ZO
NS	ZO	NS	NM	NM	NS	NS	ZO
ZO	ZO	NS	NS	NS	NS	NS	ZO
PS	ZO	ZO	ZO	ZO	ZO	ZO	ZO
PM	PB	NS	PS	PS	PS	PS	PB
PB	PB	PM	PM	PM	PS	PS	PB

From Figure 3, the transfer function of the F-PID control system is as follows:

$$\begin{aligned} G^*(s) &= G_1(s) * G(s) \\ &= \frac{K_d's^2 + K_p's + K_i'}{s} * \frac{0.07128}{(s+0.0954)(s+0.34)} \\ &= \frac{0.07128\left(K_d's^2 + K_p's + K_i'\right)}{s(s+0.0954)(s+0.34)} \end{aligned} \tag{13}$$

where $G(s)$ can be obtained from Formula 7, $G_1(s)$ is the transfer function of the F-PID controller, and the state-space expression of the system is:

$$\begin{cases} \begin{bmatrix} \dot{x_1} \\ \dot{x_2} \\ \dot{x_3} \end{bmatrix} = \begin{bmatrix} a_{11} & a_{12} & a_{13} \\ a_{21} & a_{23} & a_{23} \\ a_{31} & a_{32} & a_{33} \end{bmatrix} \begin{bmatrix} x_1 \\ x_2 \\ x_3 \end{bmatrix} \\ u = \begin{bmatrix} 1 & 1 & 1 \end{bmatrix} \begin{bmatrix} x_1 \\ x_2 \\ x_3 \end{bmatrix} \end{cases} \tag{14}$$

where $a_{11} = a_{12} = a_{13} = -2.2K_i'$,
$a_{21} = -0.2914K_p' + 3.0581K_i' + 0.0276K_d'$,
$a_{21} = -0.2914K_p' + 3.0581K_i' + 0.0276K_d' + 0.954$,
$a_{21} = -0.2914K_p' + 3.0581K_i' + 0.0276K_d'$,
$a_{31} = 0.2914K_p' - 0.8581K_i' - 0.989K_d'$,
$a_{32} = 0.2914K_p' - 0.8581K_i' - 0.989K_d'$,
$a_{33} = 0.2914K_p' - 0.8581K_i' - 0.989K_d' + 0.34$.

B. PREDICTIVE CONTROL SYSTEM DESIGN

Predictive control mainly includes model prediction and rolling optimization steps. Many predictive control methods are available. In this study, the state-space prediction algorithm is used. Compared with the traditional model prediction algorithm, the state-space prediction algorithm does not need to solve the Diophantine equation online, and it is more concise in the single-input single-output equation.

1) STATE-SPACE PREDICTION MODEL

The basic ideas of predictive control are to predict future dynamics of the system based on the established system model, to obtain the local optimal solution of the system by rolling the solution, and to apply the first element of the solved solution to the controlled system. The state-space control model of the system derives the state-space model prediction equation. The equation is as follows:

$$\begin{cases} \dot{x}(t) = A_c x(t) + B_c u(t) \\ y(t) = C_c x(t) \end{cases} \tag{15}$$

where $x(t)$ is the state variable of the system, $u(t)$ is the control input variable, and $y(t)$ is the system output variable, A_c, B_c, and C_c are coefficient matrices. The discretized state-space model prediction equation is as follows:

$$\begin{cases} \triangle x(k+1) = A\triangle x(k) + B\triangle u(k) \\ y(k) = C\triangle x(k) + y(k-1) \end{cases} \tag{16}$$

where $A = e^{A_c T_s}$, $B = \int_0^{T_s} e^{A_c T_s} * B_c$, $C = C_c$, T_s is the sampling time, $\triangle x(k)$ can be obtained as follows:

$$\begin{cases} \triangle x(k) = x(k) - x(k-1) \\ \triangle u(k) = u(k) - u(k-1) \end{cases} \tag{17}$$

assuming that the control system predicts p steps forward, the control time domain of the controller is c, and $p > c$. When the value of p is relatively small, it cannot respond to sudden changes in the reference input. When the value of p is relatively large, the system's response to disturbances will slow down. Therefore, in general, the reasonable recommendation for selecting the number of prediction steps is to have 20 to 30 samples covering the open-loop transient system response, and the control step length is generally 10%-20% of the prediction range. This article takes the number of predicted steps as 20 and the number of control steps as 4. The system predicts the incremental value of p steps at time

k as follows:

$$\begin{cases} \triangle x\,(k+1|k) = A\triangle x\,(k) + B\triangle u\,(k) \\ \triangle x\,(k+2|k) = A\triangle x\,(k+1) + B\triangle u\,(k+1) \\ \qquad\qquad = A^2\triangle x\,(k) + AB\triangle u\,(k) \\ \qquad\qquad\quad + B\triangle u\,(k+1) \\ \triangle x\,(k+3|k) = A\triangle x\,(k+2) + B\triangle u\,(k+2) \\ \qquad\qquad = A^3\triangle x\,(k) + A^2B\triangle u\,(k) \\ \qquad\qquad\quad + AB\triangle u\,(k+1) + B\triangle u\,(k+2) \\ \vdots \\ \triangle x\,(k+c|k) = A\triangle x\,(k+c-1) + B\triangle u\,(k+c-1) \\ \qquad\qquad = A^c\triangle x\,(k) + A^{c-1}B\triangle u\,(k) \\ \qquad\qquad\quad + A^{c-2}B\triangle u\,(k+1) + \cdots \\ \qquad\qquad\quad + AB\triangle u\,(k+c-2) \\ \qquad\qquad\quad + B\triangle u\,(k+c-1) \\ \vdots \\ \triangle x\,(k+p|k) = A\triangle x\,(k+p-1) + B\triangle u\,(k+p-1) \\ \qquad\qquad = A^p\triangle x\,(k) + A^{p-1}B\triangle u\,(k) \\ \qquad\qquad\quad + A^{p-2}B\triangle u\,(k+1) + \cdots \\ \qquad\qquad\quad + A^{p-c}B\triangle u\,(k+c-1) \end{cases} \tag{18}$$

Similarly, the system predicts that the output of step p at time k is:

$$\begin{cases} y\,(k+1|k) = C\triangle x\,(k+1|k) + y\,(k) \\ \qquad\qquad = CA\triangle x\,(k) + CB\triangle u\,(k) + y\,(k) \\ y\,(k+2|k) = C\triangle x\,(k+2|k) + y\,(k+1|k) \\ \qquad\qquad = \left(CA^2 + CA\right)\triangle x\,(k) \\ \qquad\qquad\quad + (CAB + CB)\triangle u\,(k) \\ \qquad\qquad\quad + CB\triangle u\,(k+1) + y\,(k) \\ \vdots \\ y\,(k+c|k) = C\triangle x\,(k+c|k) + y\,(k+c-1|k) \\ \qquad\qquad = \sum_{i=1}^{c} CA^i\triangle x\,(k) + \sum_{i=1}^{c} CA^{i-1}B\triangle u\,(k) \\ \qquad\qquad\quad + \sum_{i=1}^{c-1} CA^{i-1}B\triangle u\,(k+1) + \cdots \\ \qquad\qquad\quad + CB\triangle u\,(k+c-1) + y\,(k) \\ \vdots \\ y\,(k+p|k) = C\triangle x\,(k+p|k) + y\,(k+p-1|k) \\ \qquad\qquad = \sum_{i=1}^{p} CA^i\triangle x\,(k) + \sum_{i=1}^{p} CA^{i-1}B\triangle u\,(k) \\ \qquad\qquad\quad + \sum_{i=1}^{p-1} CA^{i-1}B\triangle u\,(k+1) + \cdots \\ \qquad\qquad\quad + \sum_{i=1}^{p-c+1} CA^{i-1}B\triangle u\,(k+c-1) + y\,(k) \end{cases} \tag{19}$$

Expression of the above derivation results in a matrix:

$$Y\,(k+1|k) = \varphi\triangle x\,(k) + \gamma y\,(k) + \tau\triangle U\,(k) \tag{20}$$

where $Y\,(k+1|k) = \begin{bmatrix} y\,(k+1|k) \\ \vdots \\ y\,(k+p|k) \end{bmatrix}$, $\gamma = \begin{bmatrix} 1 \\ \vdots \\ 1 \end{bmatrix}$

$\triangle U\,(k) = \begin{bmatrix} \triangle u\,(k) \\ \vdots \\ \triangle u\,(k+c-1) \end{bmatrix}$, $\varphi = \begin{bmatrix} CA \\ \vdots \\ \sum_{i=1}^{p} CA^i \end{bmatrix}$, and

$$\tau = \begin{bmatrix} CB & 0 & 0 & \cdots & 0 \\ \sum_{i=1}^{2} CA^{i-1}B & CB & 0 & \cdots & 0 \\ \vdots & \vdots & \vdots & \vdots & \vdots \\ \sum_{i=1}^{c} CA^{i-1}B & \sum_{i=1}^{c-1} CA^{i-1}B & \cdots & \cdots & CB \\ \vdots & \vdots & \vdots & \vdots & \vdots \\ \sum_{i=1}^{p} CA^{i-1}B & \sum_{i=1}^{p-1} CA^{i-1}B & \cdots & \cdots & \sum_{i=1}^{p-c+11} CA^{i-1}B \end{bmatrix}.$$

2) ROLLING OPTIMIZATION

The output of the controlled train system is affected by the control increment and the model dynamic coefficient. The control increment of the system is obtained by solving the optimization criterion function. For this paper, we hope that the output of the prediction controller is close to the ideal target speed curve. Then, the objective function expression can be expressed as follows:

$$J(x\,(t), \triangle U\,(k), c, p) = \|\mu_1\,(Y\,(k+1|k)) - R\,(k+1)\|^2 + \|\mu_2\triangle U\|^2 \tag{21}$$

in the formula, the weighted value matrix and the weighted value matrix with a control increment of the predictive control output error of μ_1 and μ_2 systems can be either a constant value or a time-varying matrix. For the convenience of calculation, the constant value matrix, $R\,(k+1)$ is the target output of the system.

Therefore, the optimization problem of predictive control can be expressed using the following formula:

$$min\,J(x\,(t), \triangle U\,(k), c, p) \tag{22}$$

Extreme value conditions are available, as shown below.

$$\frac{\partial\,(J(x\,(t), \triangle U\,(k), c, p))}{\partial(\triangle U(k))} = 0 \tag{23}$$

Then, the local optimal solution at the k^{th} moment can be obtained as follows:

$$\triangle U\,(k) = \left(\tau^T\mu_1^T\mu_1 + \mu_2^T\mu_2\right)^{-1}\tau^T\mu_1^T\mu_1 E_P\,(k+1|k) \tag{24}$$

in the formula, $E_P\,(k+1|k) = R\,(k+1) - \varphi x\,(k) - \gamma y\,(k)$ because the calculation of the formula is the local optimal solution of the system obtained in the open-loop state at time k. The system itself will be disturbed by many uncertain factors; consequently, the solution obtained cannot meet the requirements of tracking the target curve well. The system

must introduce feedback. Then, the real-time control increment of the closed-loop system can be expressed as follows:

$$\begin{aligned}\triangle u(k) &= \begin{bmatrix}1 & 0 & \cdots & 0\end{bmatrix} * \triangle U(k) \\ &= \begin{bmatrix}1 & 0 & \cdots & 0\end{bmatrix} \\ &\quad * \left(\tau^T \mu_1^T \mu_1 + \mu_2^T \mu_2\right)^{-1} \tau^T \mu_1^T \mu_1 \\ &\quad * E_P(k+1|k)\end{aligned} \tag{25}$$

The system rolling optimization can be expressed via the following steps:

Rolling Optimization

1: Initialization: Set the predicted step number p and control step number c, the initial value $u(0) = 0, x(0) = 0$.
2: When $k > 0$, you can get $x(k)$, calculate $y(k)$ and $\triangle x(k)$.
3: Calculate system error $E_P(k+1|k)$.
4: Calculating the real-time control increment $\triangle u(k)$ of the system by Formula 25.
5: Apply system control variable $u(k) = u(k-1) + \triangle u(k)$ to the system.
6: Get $k+1$ at time $x(k+1)$, let $k = k+1$, and return to step 2

C. ONLINE OPTIMIZATION ALGORITHM DESIGN

In this subsection, we divide the input of the control system into two parts, namely, the ideal and predictive speed curves, to track the ideal speed curve. These curves are combined in a certain proportion as the system input. An online optimization algorithm of the improved steepest descent method is proposed to solve the optimal weight of the two methods. The objective optimization function is as follows:

$$\begin{aligned}\min_m e(m) = \sum &|u(Y((k+1)|k)m + R(k+1)(1-m)) \\ &- R(k+1)|\end{aligned} \tag{26}$$

where m is weighting coefficient, $\min_m e(m)$ represents the value of m when the error is the smallest. The smaller the tracking error of the system, the better the tracking effect of the controller. Therefore, when $e(m)$ is the smallest, the control effect is the best. $u(Y((k+1)|k)m + R(k+1)(1-m))$ represents the actual speed of the suspended permanent magnetic maglev train in the k^{th} sampling period. $Y((k+1)|k)$ and $R(k+1)$ represent the output of the predictive control algorithm and expected speed of the suspended permanent magnetic maglev train in the k^{th} sampling period, respectively. From Formula 26, the gradient $\nabla e(m_a)$ of the system can be solved. After obtaining the gradient of the system, this study uses the improved steepest descent method to optimize the value of the weight m online. The following formula expresses the online optimization of m:

$$m_{a+1} = m_a - \sigma_a \nabla e(m_a) \tag{27}$$

where σ_a is the updated step size. When $\nabla e(m_a) * \nabla e(m_a+1) > 0$,the step size is doubled. In contrast, the step size becomes half that of the original. The algorithm steps are described as follows:

Online Optimization Algorithm

1: Select the initial point $m_1 = 0.5$. Given the search direction allowable error $e > 0$, the initial step size $\sigma_1 = 0.1$, the highest number of iterations $w = 1000$, and set $a = 1$.Where k is the iteration algebra
2: if $a \leq w$:
3: Calculate the search direction $d_a = -\nabla e(m_a)$.
4: if $\|d_a\| \leq e$:
5: m_a is the optimal solution, stop iterating and return to m_a.
6: else:
7: if $d_a * d_{a-1} > 0$:
8: $\sigma_a = *\sigma_{a-1}$
9: else:
10: $\sigma_a = \frac{1}{2} * \sigma_{a-1}$
11: end if.
12: Calculate $m_{a+1} = m_a - \sigma_a * \nabla e(m_a)$.
13: Calculate $\|d_{a+1}\|$.
14: end if.
15: $a = a+1$, $\|d_a\| = \|d_{a+1}\|$.
16: return to 3.
17: end if.

IV. EXPERIMENTAL SIMULATION ANALYSIS

Subsection A describes the structure of and data for the WM-F-PID controller simulation platform. The performance of the PID, F-PID, MPC, simple cascade M-F-PID and WM-F-PID controllers is compared in Subsection B, and the performance of the WM-F-PID controller is analyzed in detail. The robustness of the system with complex speed-limit is verified in Subsection C. In section D, the robustness and sensitivity of the system are verified by adding step disturbances and large-scale changes in system parameters.

TABLE 4. Parameters of the medium and low speed maglev train.

Parameter	Value
Train quality$\backslash t$	1.7
Train length$\backslash m$	3
Maximum running speed ($Km\backslash h$).	120
Maximum $F\backslash N$.	2100
Maximum acceleration($m\backslash s^2$).	0.8
Maximum acceleration($m\backslash s^2$).	-0.8
Suspension height(mm).	20∼32

A. SIMULATION PLATFORM AND DATA

The ATO speed-tracking control scenario for suspended permanent magnetic maglev trains from Jiangxi University of Science and Technology is chosen as the experimental simulation object. The train Operation and Suspension Diagram is shown in Figure 4. The specific parameters of the medium and low speed suspended permanent magnetic maglev train

FIGURE 4. Operation and suspension diagram of permanent magnetic maglev train.

are shown in Table 4. A set of speed-tracking control simulation platforms for suspended permanent magnetic maglev trains is designed. The track information for a section of the Jinan-Xuzhou high-speed railway is used to design the ideal target speed curve of the train. The simulation platform contains detailed train operation information, such as a train running speed, acceleration, position, speed-limit, track slope, and turning radius. The real-time speed of the train is calculated by processing the unit through a photoelectric speed sensor, Doppler speed measuring radar, and accelerometer. The system redundancy can be increased to obtain more accurate real-time train speed information by using various speed sensors. The acceleration of the train is measured by the accelerometer. At present, the positioning system of the suspended permanent magnetic maglev train experimental line consists of the cross-loop line, the on-board antenna box, the carrier generator, and the address detection unit. The carrier signal of 48 *kHz* generated by the carrier generator is sent to the cross-loop line through the on-board antenna box, and the address detection unit senses different phase changes in the cross-loop line to obtain the train position information through calculation. Information such as speed-limit, track slope, and turning radius can be obtained according to the line information.

A comprehensive experimental platform is established in *MATLAB*/*Simulink* to evaluate the performance of the WM-F-PID controller, as shown in Figure 5:

From Figure 5, the system includes four main modules. Input module: This module mainly includes the offline and online data for train operation. The offline data include speed-limit data, ramp data, curve data, ideal-speed data, and other information. The online data include the running speed, location, and other information about the train. Control module: This module contains the control algorithm proposed

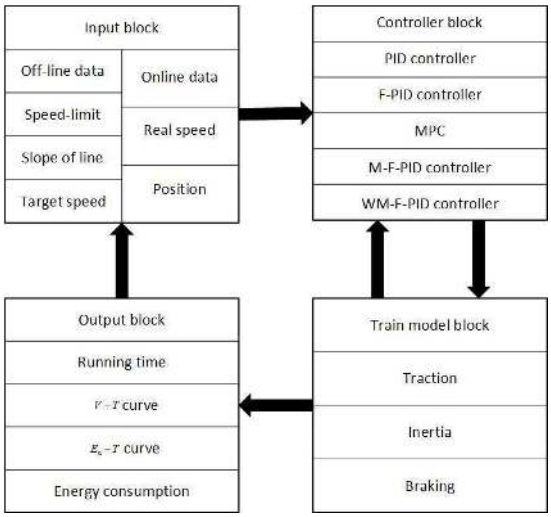

FIGURE 5. Simulation platform for WM-F-PID controller.

in this article and several other comparison algorithms, such as the PID, F-PID, MPC, simple cascade MF-PID, and WM-F-PID control algorithms. Train module: This module contains three main operating states of the train, namely, traction, inert, and deceleration states. Data display module: This module mainly displays the train operation information, including actual speed, running time, and running energy consumption.

B. COMPARATIVE ANALYSIS WITH A SIMPLE SPEED-LIMIT

This subsection discusses the performance indexes of the train WM-F-PID control algorithm under the standard speed-limit conditions and compares it with the PID, F-PID, MPC, and simple cascade M-F-PID control

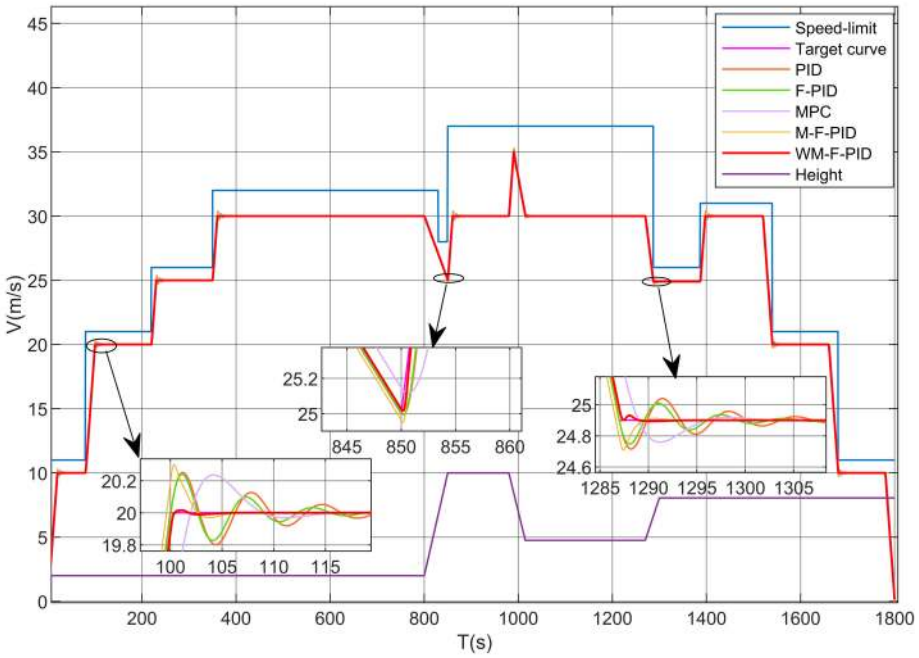

FIGURE 6. Comparison of train speed-tracking under simple speed-limit.

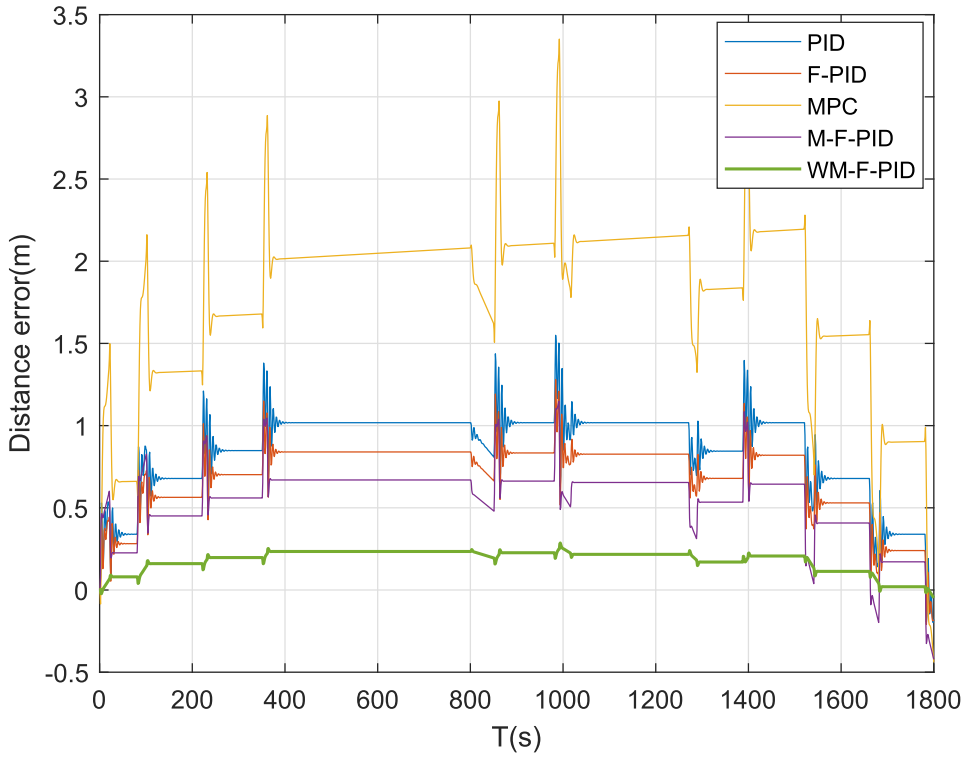

FIGURE 7. Comparison of distance error under simple speed-limit.

algorithms to verify the effectiveness of the proposed controller. The speed-time comparison curves of these control algorithms are shown in Figure 6, and the distance error comparison curves are shown in Figure 7.

As Figure 6 shows, the speed-time curves for the PID and F-PID are very similar. The PID and F-PID algorithms have larger overshoots and longer adjustment times. Although the MPC effectively reduces the system adjustment time and

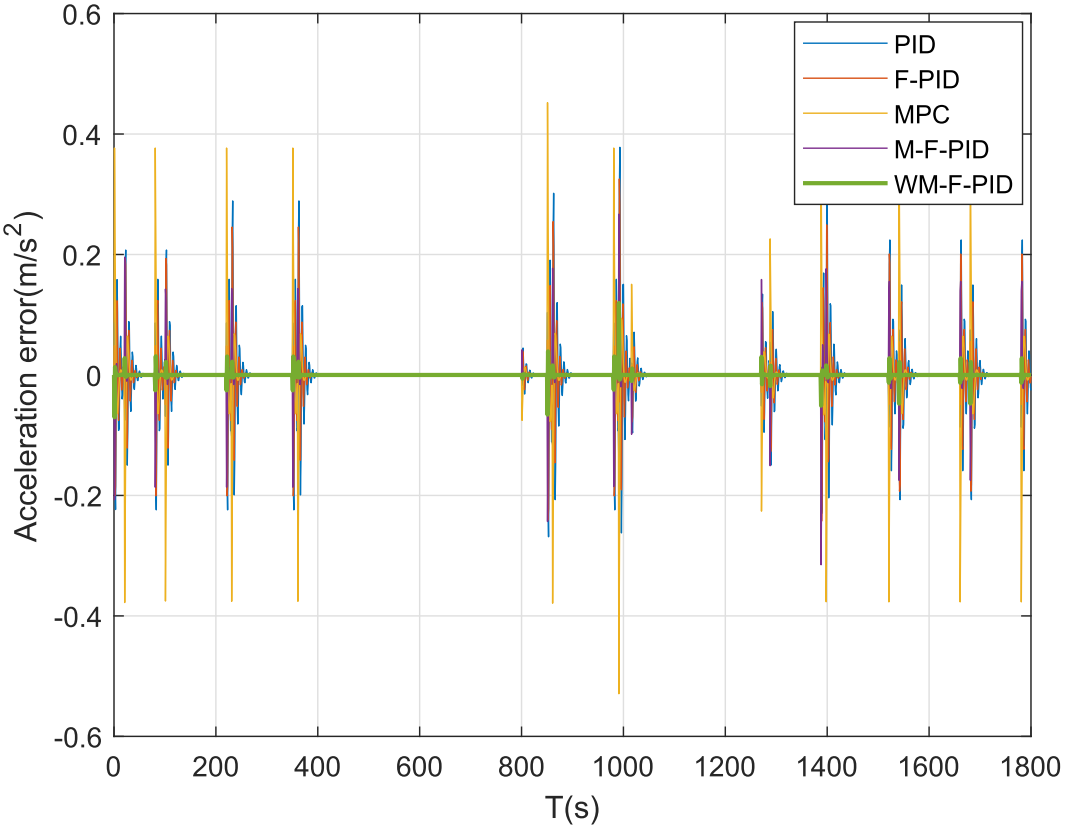

FIGURE 8. Comparison of distance error under simple speed-limit.

overshoot, the tracking error of the system is relatively large due to the slow response of the system. The simple cascaded M-F-PID control algorithm can further shorten the system adjustment time, but the system overshoot is still relatively large. In Figure 7, the displacement error of the WM-F-PID control algorithm is much smaller than that of the other four control algorithms, and the variation range of the train displacement error is relatively small. The result illustrates the good tracking effect of the algorithm from the side. A comparison of the train acceleration error curves is shown in Figure 8. PID and F-PID controller outputs switch frequently. Although the switching frequency of the MPC and simple cascade M-F-PID controllers has been reduced, the acceleration error is still large. However, the output of the WM-F-PID controller is stable and rapid, which means that the WM-F-PID control algorithm helps to improve passengers' riding comfort, reduce train operation energy consumption, and extend the life of train speed control systems.

The performance of the five controllers is calculated using Equation 8-12, and the results are shown in Table 5. The ideal controller parking error is zero. However, the actual parking error is not zero. Therefore, the smaller the train stopping error, the better the control effect of the controller. The parking errors of PID and F-PID control algorithms are relatively close. Both are less than 30 *cm*, which basically

TABLE 5. The performance comparison of the four controllers.

Algorithm	$E_u(m)$	$C_r(m\backslash s^2)$	$E_p(Kj\backslash Kg)$	N_c
PID	0.1803	0.0205	2.1970	142
F-PID	0.2174	0.0174	2.0753	136
MPC	0.6015	0.0092	1.8614	41
M-F-PID	0.4336	0.0110	1.9405	27
WM-F-PID	**0.0296**	**0.0062**	**1.7881**	**21**

meets the requirements of parking accuracy. The parking errors of MPC and simple cascade M-F-PID control algorithms are higher than the specified accuracy requirements, and the parking safety of trains cannot be guaranteed. The parking error of the WM-F-PID control algorithm is only 3 *cm*, which not only meets the parking requirements of ordinary platforms but also meets the parking requirements of platforms with screen doors. The actual track inevitably has ramps, tunnels, and curves. Therefore, the running state of the train will change. If the operation state changes dramatically, the change will bring discomfort to passengers. The smaller the comfort is, the more stable the change in train operation state is, and the better the passenger experience is, as shown in Table 5. The degree of comfort of the WM-F-PID control algorithm is much lower than that of the other four control algorithms, and the riding experience of passengers is improved. During the operation of a suspended

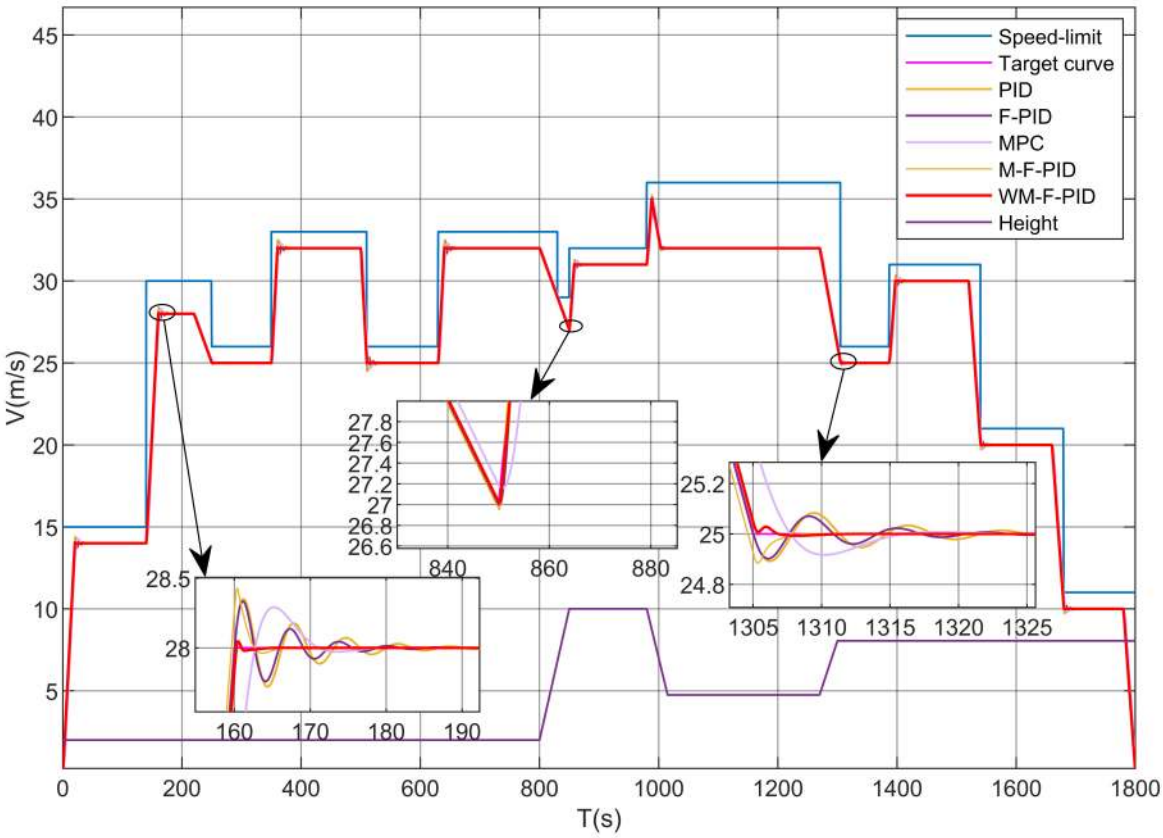

FIGURE 9. Comparison of train speed-tracking under complex speed-limit.

permanent magnetic maglev train, traction and braking will consume considerable energy. We are committed to designing an optimal speed-tracking controller to reduce unnecessary energy consumption, as shown in Table 5. Compared with the PID, F-PID, MPC, and simple cascade M-F-PID control algorithms, the WM-F-PID control algorithm reduces energy consumption per unit mass by 18.6%, 13.8%, 3.9% and 7.8%, respectively, which is more conducive to saving energy. When the running status of the train changes, the controller will continuously switch operations to reduce errors and accurately track the ideal speed of the train. The fewer the number of operational transitions is, the lower the energy consumption of the train, the better passengers' riding comfort, and the longer the service life of the train operation system. This condition is demonstrated in Table 5. The WM-F-PID control algorithm can track the ideal train speed with only a dozen adjustments. Compared with PID and F-PID, these measures are reduced nearly $7 - fold$, and compared with MPC and simple cascade M-F-PID by $1.9 - fold$ and $1.2 - fold$, respectively. In summary, the algorithm can not only track the ideal speed accurately in real-time but can also significantly improve the parking error, energy-saving, and good passengers' riding comfort.

C. COMPARATIVE ANALYSIS WITH A COMPLICATED SPEED-LIMIT

Many uncertain factors, such as weather conditions, line problems, equipment issues, and emergencies, occur in the train operation process. The train dispatcher will temporarily issue train speed-limit commands in accordance with different situations to ensure the safe and efficient operation of the train. This section verifies the adaptability of the controller under complex speed-limit conditions in emergencies. A comparison of speed-time curves under complex speed-limit conditions is shown in Figure 9, a comparison of distance error curves is shown in Figure 10, and a comparison of train acceleration error curves is shown in Figure 11. The performance of the five controllers calculated using Formulas 8-12 is shown in Table 6.

Figures 9-11 and Table 6 show that the performance indicators of PID and F-PID control algorithms basically result in the safe operation of vehicles following complex speed-limit. The MPC and simple cascaded M-F-PID control algorithms are far superior to PID and F-PID in terms of passenger comfort, energy consumption, and switching frequency. However, the MPC control algorithm is inferior to several other control algorithms in terms of real-time performance and

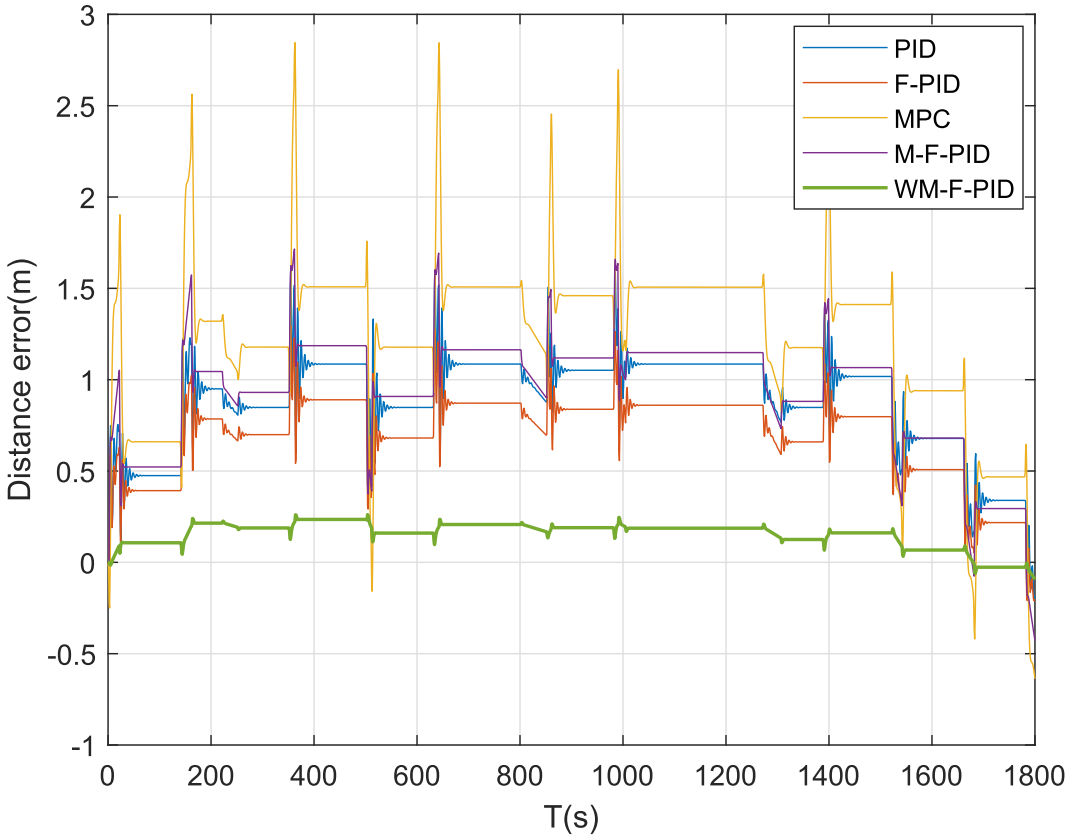

FIGURE 10. Comparison of train distance error under complex speed-limit.

TABLE 6. The performance comparison of the four controllers.

Algorithm	$E_u(m)$	$C_r(m\backslash s^2)$	$E_p(Kj\backslash Kg)$	N_c
PID	0.1805	0.0253	2.9177	175
F-PID	0.2395	0.0219	2.7801	162
MPC	0.6296	0.0092	2.4830	51
M-F-PID	0.4475	0.0138	2.5751	36
WM-F-PID	**0.0478**	**0.0082**	**2.3701**	**30**

parking error and cannot guarantee the safety of the train. Compared with the MPC control algorithm, the simple cascaded M-F-PID control algorithm has better parking error and lower switching frequency, but the parking error of the simple cascaded M-F-PID control algorithm is still higher than the parking error standard (the standard parking error should be within 30 *cm*). In contrast, the control method proposed in this paper is significantly better than the other four control algorithms in terms of real-time performance, parking error, comfort, energy consumption and switching frequency. Therefore, the control algorithm is a feasible, effective and efficient speed-tracking control scheme for medium and low speed suspended permanent magnetic maglev trains.

D. ROBUSTNESS AND SENSITIVITY ANALYSIS

In the simulation system analysis of the first two sections, the WM-F-PID control algorithm can adapt to different speed limits. In this section, we will verify the robustness of the WM-F-PID speed tracking control algorithm under uncertain interference. We introduced step signals with amplitudes of 0.2 and -0.2 as external interference signals at 700 s and 1100 s, respectively. The simulation curves of the PID, F-PID, simple cascade MPC, simple cascade M-F-PID, and WM-W-PID controllers return to a stable state after being disturbed, as shown in Figure 12.

Figure 12 shows that the PID, F-PID, simple cascade M-F-PID and WM-F-PID methods can all return to a stable state after being disturbed by the outside world. However, the output switching frequency, adjustment time and fluctuation range of the PID, F-PID and simple cascade M-F-PID control algorithms are much higher than those of the WM-F-PID control algorithm. Although the MPC control algorithm has a smaller switching frequency and fluctuation range, the adjustment time is almost twice that of the WM-F-PID control algorithm, and the real-time system is relatively poor. This observation verifies that the WM-F-PID control algorithm has a good control effect and robustness.

However, the above simulation experiment cannot prove the sensitivity of the control system when the parameters of the control system are changed over a wide range. Therefore, the following simulation experiment was designed: the parameters of the PID controller were changed to half that

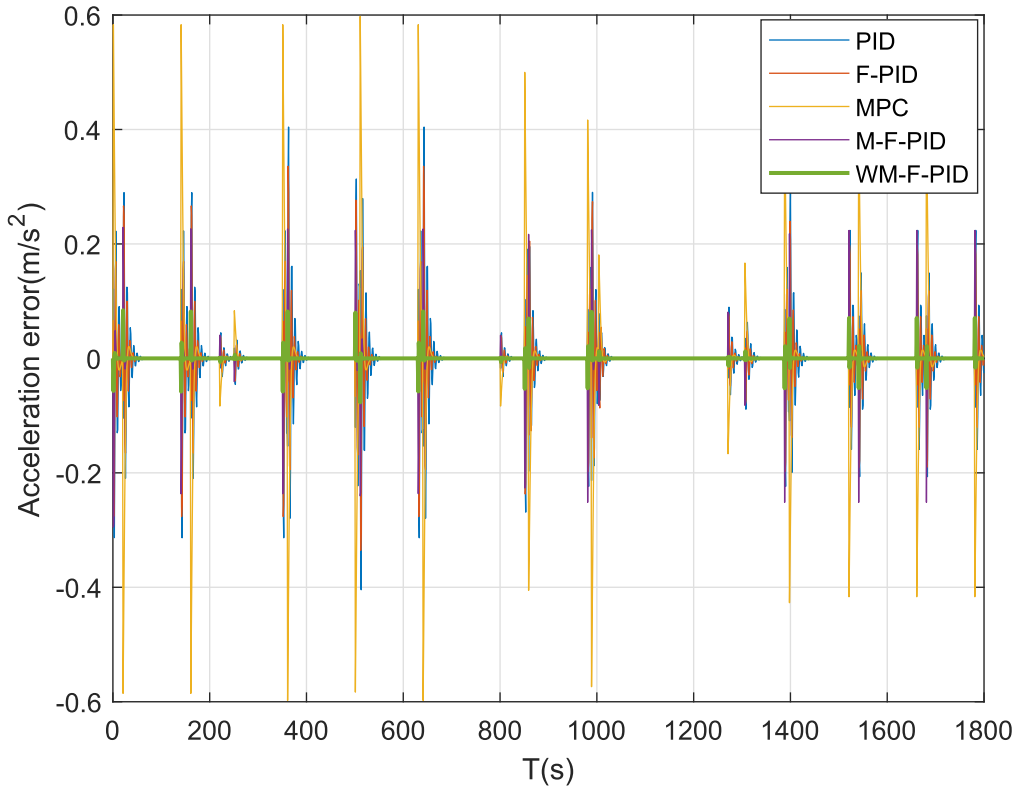

FIGURE 11. Comparison of train acceleration error under complex speed-limit.

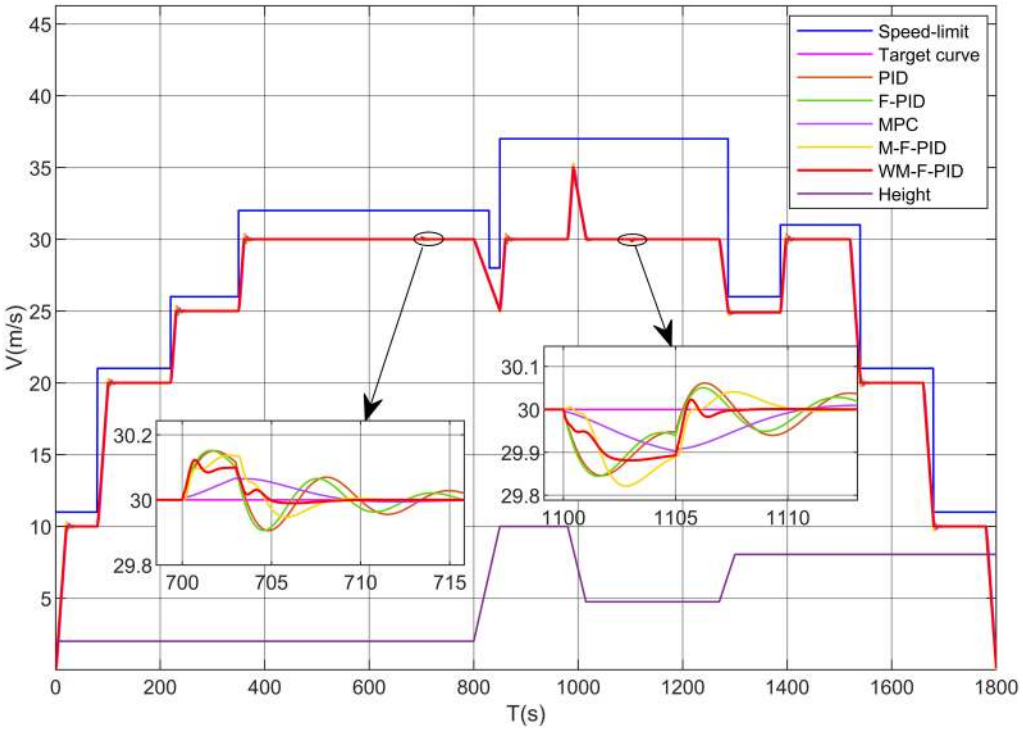

FIGURE 12. Robustness analysis of simple speed-limit.

of the original, and the control effects of the PID, F-PID, simple cascade M-F-PID, and WM-F-PID control algorithms were compared to verify the WM-F-PID control algorithm sensitivity.

As shown in Figure 13, the WM-F-PID control algorithm proposed in this paper still has a better control effect than other algorithms. Therefore, the WM-F-PID control algorithm proposed in this paper has strong robustness.

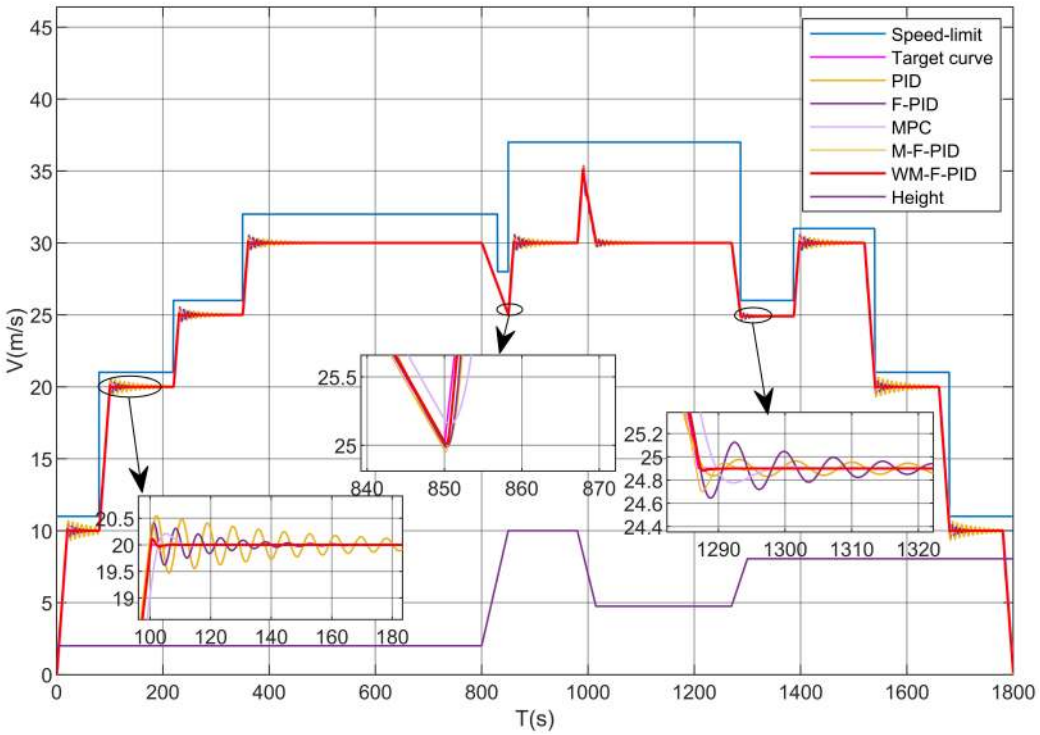

FIGURE 13. Sensitivity analysis under a wide range of parameters.

V. CONCLUSION

This paper proposes a cascaded WM-F-PID control algorithm to address the speed-tracking control problem for the suspended permanent magnet maglev train to system time delays and uncertain interference. More specifically, the proposed cascaded WM-F-PID speed-tracking controller includes a two-layer algorithm structure: the predictive control algorithm of the outer layer and the fuzzy PID control algorithm of the inner layer. The input of the internal fuzzy PID control algorithm is the mixing speed that combines the output of the external predictive control algorithm with the ideal input according to a certain weight. In order to accurately solve the weight of the predicted speed under mixed speed in real-time, an improved steepest descent algorithm is proposed.The simulation experiment results under the MATLAB/Simulink simulation platform show that compared with the traditional speed-tracking control algorithm based on PID, F-PID, MPC and simple cascade M-F-PID, train operation by the WM-F-PID control algorithm results in reduced energy consumption by up to 18.6%, a reduced number of output changes by up to $7 - fold$, a reduced parking error of less than 5 cm, and an improvement in passenger comfort of 69%. The WM-F-PID control algorithm proposed in this paper has better performance, especially in terms of energy consumption, controller output conversion times, parking error and passenger comfort. This study also uses different train speed-limits, different slopes, uncertain interference and wide-ranging changes in parameters to perform simulations, indicating that the method has good robustness.

However, due to the relatively large numbers of calculations and low computational efficiency of the predictive control algorithm, this control algorithm is only suitable for the speed control system of medium and low speed trains. In future work, we will optimize the computational complexity of the model predictive controller to suit the needs of high-speed permanent magnet maglev trains. Of course, the algorithm is not only suitable for medium and low speed permanent magnet maglev trains but also for other medium and low speed passenger trains and freight trains, as well as the auto-driving path tracking of automobiles. This area of future study will be interesting.

REFERENCES

[1] S. Gao, H. Dong, B. Ning, Y. Chen, and X. Sun, "Adaptive fault-tolerant automatic train operation using RBF neural networks," *Neural Comput. Appl.*, vol. 26, no. 1, pp. 141–149, Jan. 2015.

[2] M. Ganesan, D. Ezhilarasi, and J. Benni, "Hybrid model reference adaptive second order sliding mode controller for automatic train operation," *IET Control Theory Appl.*, vol. 11, no. 8, pp. 1222–1233, May 2017.

[3] J. Yin, T. Tang, L. Yang, J. Xun, Y. Huang, and Z. Gao, "Research and development of automatic train operation for railway transportation systems: A survey," *Transp. Res. C, Emerg. Technol.*, vol. 85, pp. 548–572, Dec. 2017.

[4] X. Chen, W. Ma, G. Xie, X. Hei, and F. Wang, "A survey of control algorithm for automatic train operation," in *Proc. 14th IEEE Conf. Ind. Electron. Appl. (ICIEA)*, Xi'an, China, Jun. 2019, pp. 2405–2410.

[5] M. Dominguez, A. Fernandez-Cardador, A. P. Cucala, and R. R. Pecharroman, "Energy savings in metropolitan railway substations through regenerative energy recovery and optimal design of ATO speed profiles," *IEEE Trans. Autom. Sci. Eng.*, vol. 9, no. 3, pp. 496–504, Jul. 2012.

[6] J. Yang, L. Jia, S. Lu, Y. Fu, and J. Ge, "Energy-efficient speed profile approximation: An optimal switching region-based approach with adaptive resolution," *Energies*, vol. 9, no. 10, pp. 1–27, OCT. 2016.

[7] X. Yang, X. Li, B. Ning, and T. Tang, "A survey on energy-efficient train operation for urban rail transit," *IEEE Trans. Intell. Transp. Syst.*, vol. 17, no. 1, pp. 2–13, Jan. 2016.
[8] X. Zhuan and X. Xia, "Brief paper: Speed regulation with measured output feedback in the control of heavy haul trains," *Energies*, vol. 9, no. 10, pp. 1–27, OCT. 2016.
[9] W. ShangGuan, X.-H. Yan, B.-G. Cai, and J. Wang, "Multiobjective optimization for train speed trajectory in CTCS high-speed railway with hybrid evolutionary algorithm," *IEEE Trans. Intell. Transp. Syst.*, vol. 16, no. 4, pp. 2215–2225, Aug. 2015.
[10] B. Moaveni, F. R. Fathabadi, and A. Molavi, "Supervisory predictive control for wheel slip prevention and tracking of desired speed profile in electric trains," *ISA Trans.*, vol. 101, pp. 102–115, Jun. 2020.
[11] D.-L. Yu, T. K. Chang, and D.-W. Yu, "Fault tolerant control of multivariable processes using auto-tuning PID controller," *IEEE Trans. Syst., Man, Cybern. B. Cybern.*, vol. 35, no. 1, pp. 32–43, Feb. 2005.
[12] B.-R. Ke, C.-L. Lin, and C.-W. Lai, "Optimization of train-speed trajectory and control for mass rapid transit systems," *Control Eng. Pract.*, vol. 19, no. 7, pp. 675–687, Jul. 2011.
[13] H. Shen and J. Yan, "Optimal control of rail transportation associated automatic train operation based on fuzzy control algorithm and PID algorithm," *Autom. Control Comput. Sci.*, vol. 51, no. 6, pp. 435–441, Nov. 2017.
[14] J. Yang, L. Jia, Y. Fu, and S. Lu, "Speed tracking based energy-efficient freight train control through multi-algorithms combination," *IEEE Intell. Transp. Syst. Mag.*, vol. 9, no. 2, pp. 76–90, Apr. 2017.
[15] W. Y. Liu, J. G. Han, and X. N. Lu, "A high speed railway control system based on the fuzzy control method," *Expert Syst. Appl.*, vol. 40, no. 15, pp. 6115–6124, Nov. 2013.
[16] R. Cheng, D. Chen, B. Cheng, and S. Zheng, "Intelligent driving methods based on expert knowledge and online optimization for high-speed trains," *Expert Syst. Appl.*, vol. 87, pp. 228–239, Nov. 2017.
[17] C.-Y. Zhang, D. Chen, J. Yin, and L. Chen, "A flexible and robust train operation model based on expert knowledge and online adjustment," *Int. J. Wavelets, Multiresolution Inf. Process.*, vol. 15, no. 03, May 2017, Art. no. 1750023.
[18] S. Gao, H. Dong, Y. Chen, B. Ning, G. Chen, and X. Yang, "Approximation-based robust adaptive automatic train control: An approach for actuator saturation," *IEEE Trans. Intell. Transp. Syst.*, vol. 14, no. 4, pp. 1733–1742, Dec. 2013.
[19] Y.-D. Song, Q. Song, and W.-C. Cai, "Fault-tolerant adaptive control of high-speed trains under traction/braking failures: A virtual parameter-based approach," *IEEE Trans. Intell. Transp. Syst.*, vol. 15, no. 2, pp. 737–748, Apr. 2014.
[20] B. Wang, J. Yang, H. Jiao, K. Zhu, and Y. Chen, "Design of auto disturbance rejection controller for train traction control system based on artificial bee colony algorithm," *Measurement*, vol. 160, Aug. 2020, Art. no. 107812.
[21] H. Yang, Y.-T. Fu, K.-P. Zhang, and Z.-Q. Li, "Speed tracking control using an ANFIS model for high-speed electric multiple unit," *Control Eng. Pract.*, vol. 23, pp. 57–65, Feb. 2014.
[22] Z. Li, Z. Hou, and C. Yin, "Iterative learning control for train trajectory tracking under speed constrains with iteration-varying parameter," *Trans. Inst. Meas. Control*, vol. 37, no. 4, pp. 485–493, Apr. 2015.
[23] Z. Li and Z. Hou, "Adaptive iterative learning control based high speed train operation tracking under iteration-varying parameter and measurement noise," *Asian J. Control*, vol. 17, no. 5, pp. 1779–1788, Sep. 2015.
[24] H. Oshima, S. Yasunobu, and S.-I. Sekino, "Automatic train operation system based on predictive fuzzy control," in *Proc. Int. Workshop Artif. Intell. Ind. Appl.*, Castro, Spain, June 1988, pp. 485–489.
[25] Y. Cao, L. Ma, and Y. Zhang, "Application of fuzzy predictive control technology in automatic train operation," *Cluster Comput.*, vol. 22, no. S6, pp. 14135–14144, Nov. 2019.
[26] H. Yang, Y. Fu, and D. Wang, "Multi-ANFIS model based synchronous tracking control of high-speed electric multiple unit," *IEEE Trans. Fuzzy Syst.*, vol. 26, no. 3, pp. 1472–1484, Jun. 2018.
[27] L. Wang, X. Wang, Z. Sheng, and S. Lu, "Model predictive controller based on online obtaining of softness factor and fusion velocity for automatic train operation," *Sensors*, vol. 20, no. 6, p. 1719, Mar. 2020.
[28] K.-W. Liu, X.-C. Wang, and Z.-H. Qu, "Research on multi-objective optimization and control algorithms for automatic train operation," *Energies*, vol. 12, no. 20, p. 3842, Oct. 2019.
[29] P. Chu, Y. Yu, D. Dong, H. Lin, and J. Yuan, "NSGA-II-based parameter tuning method and GM(1,1)-based development of fuzzy immune PID controller for automatic train operation system," *Math. Problems Eng.*, vol. 2020, Mar. 2020, Art. no. 3731749.
[30] H. Wang, B. Liu, X. Ping, and Q. An, "Path tracking control for autonomous vehicles based on an improved MPC," *IEEE Access*, vol. 7, pp. 161064–161073, 2019.
[31] L. Zhang and X. Zhuan, "Optimal operation of heavy-haul trains equipped with electronically controlled pneumatic brake systems using model predictive control methodology," *IEEE Trans. Control Syst. Technol.*, vol. 22, no. 1, pp. 13–22, Jan. 2014.
[32] Y. Yang, Z. Xu, W. Liu, H. Li, R. Zhang, and Z. Huang, "Optimal operation of high-speed trains using hybrid model predictive control," *J. Adv. Transp.*, vol. 2018, May 2018, Art. no. 7308058.
[33] R. Liu and I. M. Golovitcher, "Energy-efficient operation of rail vehicles," *Transp. Res. A, Policy Pract.*, vol. 37, no. 10, pp. 917–932, Dec. 2003.
[34] Q. Song, Y. D. Song, and W. Cai, "Adaptive backstepping control of train systems with traction/braking dynamics and uncertain resistive forces," *Vehicle Syst. Dyn.*, vol. 49, no. 9, pp. 1441–1454, Sep. 2011.
[35] Y. Cao, Z.-C. Wang, F. Liu, P. Li, and G. Xie, "Bio-inspired speed curve optimization and sliding mode tracking control for subway trains," *IEEE Trans. Veh. Technol.*, vol. 68, no. 7, pp. 6331–6342, Jul. 2019.
[36] L. Zhiqiang, L. Yun, and W. Xu, "On maglev train automatic operation control system based on Auto-Disturbance-Rejection control algorithm," in *Proc. 27th Chin. Control Conf.*, Jul. 2008, pp. 681–685.
[37] C. Jiaxin and P. Howlett, "A note on the calculation of optimal strategies for the minimization of fuel consumption in the control of trains," *IEEE Trans. Autom. Control*, vol. 38, no. 11, pp. 1730–1734, Nov. 1993.

YAHUI LIU (Student Member, IEEE) received the B.S. degree in transportation from the Anyang Institute of Technology, Anyang, China, in 2019. He is currently pursuing the M.S. degree in control engineering with the Jiangxi University of Science and Technology, Ganzhou, China. His current research interests include speed control of permanent magnetic maglev train, suspension control of permanent magnet maglev train, and speed optimization of permanent magnetic maglev train.

KUANGANG FAN (Member, IEEE) was born in Linyi, China, in 1981. He received the B.S., M.S., and Ph.D. degrees in instrumentation science from Jilin University, in June 2006, June 2008, and June 2011, respectively. From 2012 to 2014, he held a Postdoctoral position at the State Key Laboratory of Pattern Recognition, Institute of Automation, Chinese Academy of Sciences. From 2015 to 2016, he was a Visiting Scholar with the School of Electronics and Computer Engineering, Peking University Shenzhen Graduate School. From 2018 to 2019, he was a Visiting Scholar with the Department of Electrical and Computer Engineering, UC Davis, Davis, CA, USA. He is currently an Associate Professor of electrical and computer engineering with the Jiangxi University of Science and Technology, China. He has published more than 30 refereed articles and book chapters, and holds more than 30 invention patents. His research interests include signal processing and control engineering, including blind channel estimation and equalization, source separation, parameter estimation, and adaptive control.

QINGHUA OUYANG (Graduate Student Member, IEEE) received the B.S. degree in automation from the Jiangxi University of Science and Technology, Ganzhou, China, in 2019, where he is currently pursuing the M.S. degree in control science and engineering. His current research interest includes magnetic levitation control.